BIBECHANA
Vol. 23, No. 2, April 2026, 115–128

ISSN 2091-0762 (Print), 2382-5340 (Online)
Journal homepage: http://nepjol.info/index.php/BIBECHANA
Publisher:Dept. of Phys., Mahendra Morang A. M. Campus (Tribhuvan University)Biratnagar

Computational repurposing of 1,2,4-triazole-based Schiff bases as anticancer candidates: target-specific docking, DFT reactivity descriptors, and ADMET profiling

Kishor Bhandari, Bhushan Shakya*
Department of Chemistry, Amrit Campus, Tribhuvan University, Kathmandu, Nepal.

*Corresponding authors: Email: bhusansakya@gmail.com

Abstract
The epidermal growth factor receptor (EGFR) has become a key target for most of the researcher involved in the field of anticancer drug discovery due to its role in tumor growth and progression. A series of previously reported Schiff bases of 1,2,4-triazole (T1-T8), in this study, were chosen to evaluate their potential to inhibit EGFR by applying a number of in silico techniques. Molecular docking analysis revealed that compounds T2 and T5 exhibited comparatively stronger binding affinities (-7.236 and -7.213 kcal/mol, respectively) and formed stable interactions with key active site residues, including MET769, GLN767, THR830, and LYS721. Density functional theory analysis indicated that the compounds possess suitable electronic characteristics, as reflected by moderate HOMO-LUMO energy gaps (3.377-3.900 eV), along with favorable global reactivity descriptors such as chemical hardness and electrophilicity, supporting their interaction potential with the receptor. Molecular electrostatic potential maps further identified distinct electron-rich and electron-deficient regions contributing to binding interactions. In addition, ADMET predictions suggested favorable pharmacokinetic properties, including good oral absorption and acceptable safety profiles for most compounds. Overall, the results highlight that compounds T2 and T5 demonstrate promising computational potential as EGFR-targeted anticancer candidates; however, further experimental validation is required to confirm their biological activity.

Keywords
1,2,4 triazole-based Schiff bases, ADMET prediction, DFT analysis, EGFR inhibitor, molecular docking.

Article information
Manuscript received: February 7, 2026; Revised: March 26, 2026; Accepted: April 6, 2026
DOI https://doi.org/10.3126/bibechana.v23i2.90607

1 Introduction

Cancer is a complex disease characterized by uncontrolled cell proliferation, resistance to apoptosis, and the ability to metastasize to distant organs [1, 2]. Even though early detection and treatment methods have improved a lot, cancer is still one of the top causes of death worldwide [3].

Conventional chemotherapy may be non-specific to cancer cells. It causes severe side effects and reduced efficacy [4]. Furthermore, the emergence of resistance to cancer medications further contributes to the problem [5]. For these reasons, continuous efforts have been made to develop targeted therapies that selectively act on specific biological processes involved in cancer cell growth.

Among the various molecular targets, the epidermal growth factor receptor (EGFR) has emerged as a well-established and clinically relevant target in anticancer drug discovery. EGFR is a transmembrane receptor tyrosine kinase that regulates key cellular processes such as proliferation, differentiation, and survival [6,7]. Aberrant activation of EGFR signaling, commonly through overexpression or mutation, has been strongly associated with the initiation and progression of several types of cancers [8]. As a result, inhibition of the EGFR kinase domain, particularly at the ATP-binding site, has become an effective strategy for suppressing tumor growth and proliferation [6, 9].

Schiff bases of 1,2,4-triazole have been widely studied in the area of medicinal chemistry. This is because of their flexibility and different biological applications [10, 11]. 1,2,4-triazole ring in the molecule increase the stability and binding affinity of the compounds. This is due to its favorable electronic properties and ability to form hydrogen bonds [12]. Past reports highlight that these Schiff bases showed antimicrobial, antioxidant, and anticancer activities [13, 14]. However, the molecular interaction of these compounds with EGFR has not been investigated widely.

Computational approaches have emerged as an important component of contemporary drug discovery research, especially during the initial stages of lead identification and optimization [15]. *In silico* studies, namely molecular docking, density functional theory (DFT), and ADMET prediction, provide a rational and cost-effective solution for the early stages of drug discovery. These strategies enable the evaluation of numerous chemical compounds quickly, thereby reducing the cost and time involved before moving on to experimental studies [16, 17]. In regard, molecular docking helps in understanding the binding modes and interaction patterns, whereas DFT calculations provide information on the electronic properties and chemical reactivity of the compound [18, 19]. Similarly, ADMET prediction helps in understanding the pharmacokinetic properties and drug-likeness of the compound before experimental validation [20].

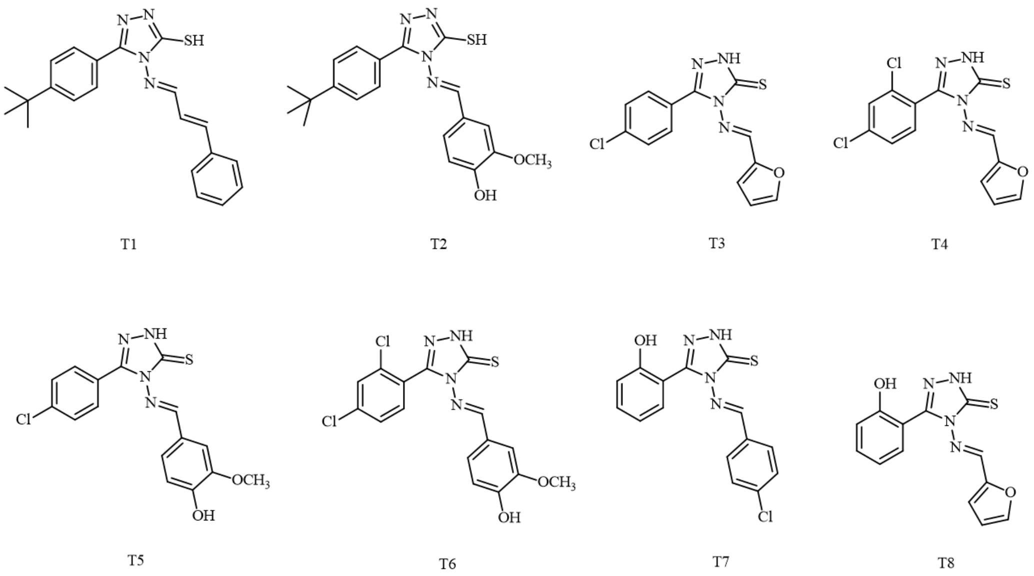

Figure 1: Chemical structures of selected 1,2,4-triazole-based Schiff bases from our previous work [21–23].

Therefore, in the current study, a set of 1,2,4-triazole Schiff bases that have already been synthesized and characterized by our research group were chosen and systematically evaluated for their potential as EGFR inhibitors using an integrated *in silico* approach [21–23], Figure 1. Although these compounds have been reported earlier for their synthesis and preliminary biological activities, their interaction with EGFR has not been explored in detail. Moreover, while computational studies on triazole derivatives have been reported, a combined investigation involving molecular docking, DFT-based reactivity descriptors, and ADMET profiling for these specific compounds is still lacking. In this context, the present work aims to provide a detailed molecular-level understanding of ligand-receptor interactions with EGFR, supported by electronic structure analysis and pharmacokinetic predictions. This integrated study is expected to offer new insights into the structure-activity relationship of 1,2,4-triazole Schiff bases and to identify promising candidates for further experimental validation as EGFR-targeted anticancer agents.

2 Materials and methods

2.1 Molecular docking

2.1.1 Protein preparation

The crystal structure of the target protein was retrieved from the Protein Data Bank (PDB ID: 1M17, Resolution = 2.60 Å) [24] and analyzed using the Molecular Operating Environment (MOE 2015) software platform [25]. Before the docking experiment, all the crystallographic water molecules, ligands, and unnecessary heteroatoms were removed. Hydrogen atoms were added, and correct protonation states of the amino acid residues were assigned at physiological pH values using the Protonate 3D module. Partial atomic charges were assigned depending on the chosen force field. To eliminate unfavorable interactions and optimize the protein structure, energy minimization was performed using the default force field, while restraining the protein backbone atoms [26]. The optimized protein structure was then used directly for molecular docking experiments in the MOE software.

2.1.2 Ligand preparation

The ligands used for the molecular docking experiment were first optimized using density functional theory (DFT) calculations employing B3LYP/6-31G(d,p) basis set. These DFT optimized molecular frameworks were confirmed as true minima on the potential energy surface by verifying the absence of negative frequencies. These optimized structures were then used for docking studies in Molecular Operating Environment (MOE 2015) software package [27]. Hydrogen atoms were added, and the protonation states were specified for biological relevance employing the Protonate 3D tool. Local strain introduced as a result of protonation was eliminated through energy minimization for a short period, retaining the DFT-optimized structures. The MMFF94x force field method was employed with an RMS gradient convergence criterion of 0.1 kcal mol^{-1} Å^{-1}. Ligand flexibility was fully considered during docking by allowing rotation of all rotatable bonds, thereby enabling exploration of relevant conformational space within the active site.

2.1.3 Docking protocol

Molecular docking calculations were performed to understand the interaction pattern between the ligands and the target protein using the Molecular Operating Environment (MOE 2015) [25]. The active sites of the protein were identified using the site finder tool, and dummy atoms were created to determine the binding pockets [28]. The docking calculation was performed using the Triangle Matcher placement algorithm. The poses of the ligands at the protein binding sites were scored using the London dG scoring function. The poses of the ligands at the protein binding sites were refined using the force field-based refinement algorithm, followed by rescoring using the GBVI/WSA dG scoring function [26]. The flexibility of the ligands during the docking calculation was allowed by rotating all the bonds of the ligands. The binding conformation of each ligand with the protein was identified based on the docking score, binding interactions, and geometric complementarity at the active sites.

2.1.4 Docking validation

The validation of docking procedure was performed by re-docking the native ligand into the active site of the target protein using MOE 2015 following the same docking parameters applied for the test compounds. After completion of the docking process, the resulting complex was structurally aligned with the corresponding experimental structure by superposition of the protein backbone. The root-mean-square deviation (RMSD) between the heavy atoms of the re-docked ligand and the co-crystallized ligand was then calculated using Biovia Discovery Studio visualizer [29–31].

2.2 Density functional theory (DFT) calculation

The DFT calculations were carried out to optimize the molecular structures and analyze the electronic properties of the chosen 1,2,4-triazole Schiff bases to explain their interaction capacity with the epidermal growth factor receptor (EGFR). All the quantum calculations were carried out using the Gaussian 09 program and GaussView 6.0 is used for the graphical interpretation. Geometry optimization was carried out using the B3LYP hybrid functional with the 6-31G(d,p) basis set [32], which is a suitable choice for balancing the accuracy and computational cost of organic drug-like molecule [17]. The optimized structures were confirmed to be true energy minima by the absence of imaginary vibrational frequencies. Frontier molecular orbital (FMO) energies, which include the highest occupied molecular orbital (HOMO) and lowest unoccupied molecular orbital (LUMO), were computed to calculate the HOMO-LUMO energy gap (ΔE). The global reactivity descriptors namely ionization potential (I), electron affinity (A), electronegativity (χ), chemical potential (μ), global hardness (η), global softness (S), and global electrophilicity index (ω) were calculated employing the following relations [17,33,34]

$$\text{Ionization Potential } (I) = -E_{\text{HOMO}} \tag{1}$$

$$\text{Electron Affinity } (A) = -E_{\text{LUMO}} \tag{2}$$

$$\text{Electronegativity } (\chi) = -\frac{(E_{\text{LUMO}} + E_{\text{HOMO}})}{2} \tag{3}$$

$$\text{Chemical potential } (\mu) = -\chi = \frac{(E_{\text{LUMO}} + E_{\text{HOMO}})}{2} \tag{4}$$

$$\text{Global hardness } (\eta) = \frac{(E_{\text{LUMO}} - E_{\text{HOMO}})}{2} \tag{5}$$

$$\text{Global softness } (S) = 1/(2\eta) \tag{6}$$

$$\text{Global electrophilicity index } (\omega) = \mu^2/(2\eta) \tag{7}$$

These descriptors were used to assess the electronic stability and reactivity of the molecules and to justify the binding affinity of the molecules toward EGFR in molecular docking experiments. Moreover, molecular electrostatic potential (MEP) maps were generated on the optimized structures to analyze the electrostatic potential and the electrophilic and nucleophilic sites of the molecules. The MEP maps were plotted on the electron density surfaces using the same level of theory. The negative electrostatic potential regions (colored red) correspond to electron-rich sites prone to electrophilic interactions. Similarly, the positive electrostatic potential regions (colored blue) indicate electron-deficient sites that is favorable for nucleophilic interaction [35]. These regions were analyzed in relation to the important amino acid residues that participate in hydrogen bonding and electrostatic interactions in the EGFR active site.

2.3 *In silico* pharmacokinetics and toxicity studies

The evaluation of pharmacokinetic properties, such as absorption, distribution, metabolism, and excretion (ADME), along with toxicity profiling, is essential in contemporary drug discovery [36]. Early assessment of these factors helps reveal possible shortcomings in candidate molecules and improves the chances of successful drug development. Early ADME and toxicity profiling can also reduce development time and costs, minimize adverse effects, and support the rational and safe use of drugs in clinical settings [3]. In this section of study, SwissADME was used to evaluate physicochemical properties, drug-likeness, and to generate the BOILED-Egg model for estimating gastrointestinal absorption and blood-brain barrier permeability. Whereas, pkCSM was applied to assess pharmacokinetic ADME and toxicity-related parameters. These predictions were performed to evaluate the suitability of the compounds as potential drug candidates [37,38].

3 Results and discussion

3.1 Molecular docking analysis

The molecular docking study was carried out to examine the binding affinity and interaction behavior of the selected 1,2,4-triazole-based Schiff base derivatives (T1-T8) with the active site of EGFR. Analysis of docking scores and interaction patterns revealed a noticeable variation in the binding affinity and interaction behavior of the compounds, revealing the effect of structural diversity on EGFR recognition, Figure 2.

Among the examined derivatives, T2 and T5 exhibited good docking score values, with values of -7.236 and -7.213 kcal/mol, respectively (Table 1), revealing a strong binding affinity with EGFR's active site compared to other derivatives. T2 and T5 formed several hydrogen bond interactions with key amino acid residues, including GLN767, GLU738, THR830, and MET769. These residues play an important role in stabilizing ligands within the EGFR active site, particularly at the ATP-binding site. In addition to hydrogen bond interactions, T5 also exhibited a π-cation interaction with LYS721, a residue known for its participation in kinase inhibitors' binding with EGFR's active site. Hydrogen bond interactions and π-cation interactions are crucial for the overall stability of the ligand-protein complex with EGFR's active site. The comparatively strong docking score observed for T5 can be attributed to this effect.

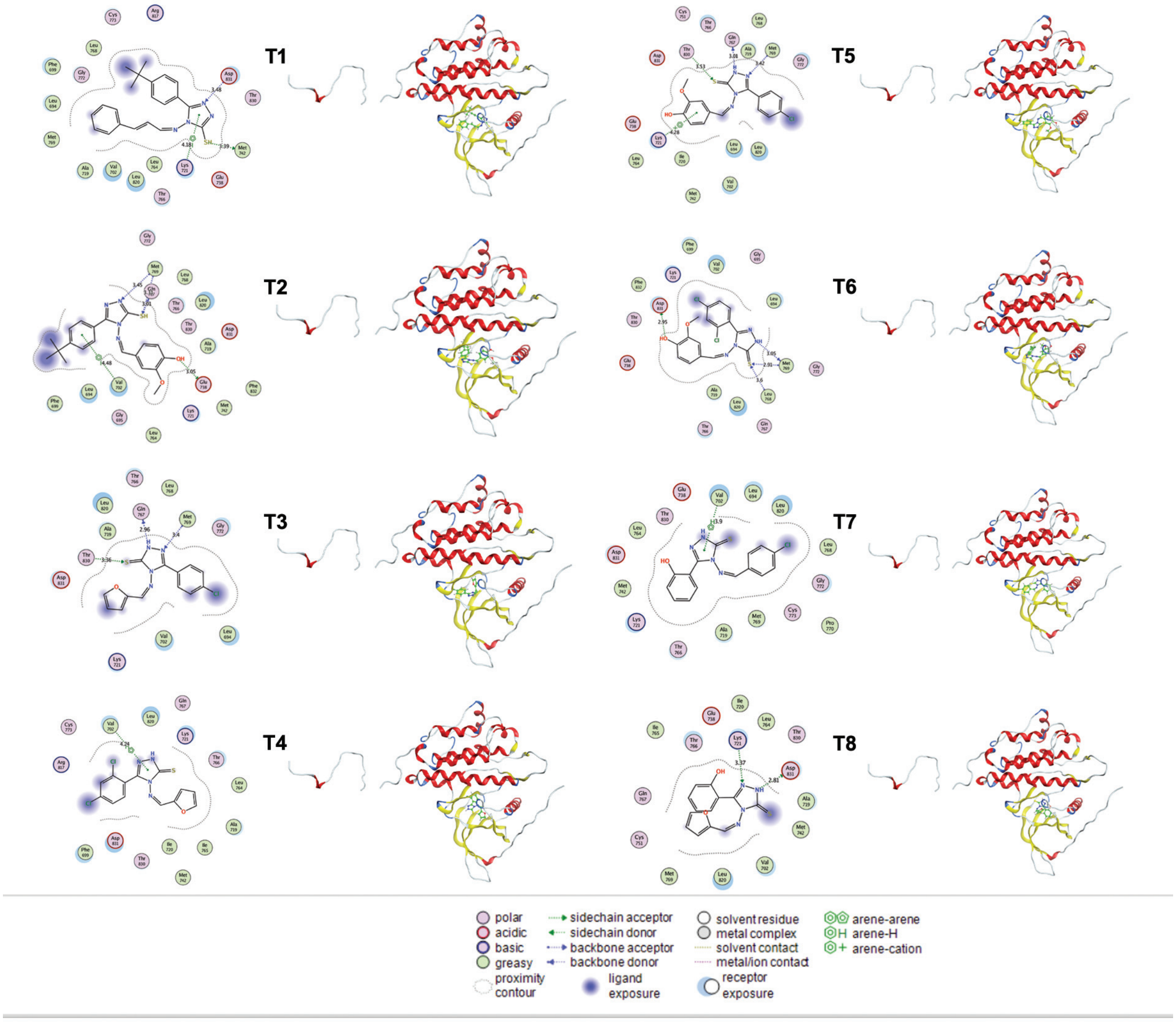

Figure 2: 2D (left) and 3D (right) plot showing the interaction between the studied compounds and the active site of the receptor protein (PDB ID: 1M17).

The interaction pattern observed for the most active compounds (T2 and T5) is consistent with that reported for established EGFR inhibitors such as erlotinib, which also form hydrogen bond interactions with MET769, GLN767, VAL702, GLU738, and THR830 within the ATP-binding pocket. The involvement of these key residues suggests that the studied compounds adopt a binding mode similar to known inhibitors. Although the docking scores of the present compounds (-7.2 kcal/mol range) are slightly lower than those typically reported for clinically used EGFR inhibitors (generally ranging from -8.5 to -9.35 kcal/mol depending on the docking protocol), the comparable interaction profiles indicate that these compounds possess a promising scaffold for further optimization [39,40].

Compound T1 had a moderate docking score of -6.927 kcal/mol. It formed hydrogen-bond interactions with MET742 and ASP831, and a π-H bond with LYS721. Despite, it formed interactions with the residues in the activation loop region (ASP831), which could be responsible for the inhibitory activity, the overall interactions of compound T1 were less complex compared to compounds T2 and T5. Compounds T3 and T6 had less potent docking scores, yet they were able to form meaningful interactions with the target. Compound T3 formed hydrogen-bond interactions with GLN767, THR830, and MET769, while compound T6 formed hydrogen-bond donor and acceptor interactions with ASP831, MET769, and LEU768. Interaction with these residues are known to play a crucial role in ligand recognition and stabilization within the ATP-binding pocket, contributing to the specificity and proper orientation of the ligand, even if the overall binding affinity is poor. The relatively lower docking scores observed for T3 and T6 may be attributed to suboptimal geometric orientation or weaker hydrophobic and π-type interactions, which are also important contributors to total binding energy. Therefore, while these compounds demonstrate the ability to engage essential residues, the lack of complementary interactions reduces their overall binding strength compared to higher-scoring compounds such as T2 and T5.

Compounds T4 and T7 had the least complex interactions with the target. Compound T4 and T7 formed π-H interactions with VAL702 and lacked hydrogen-bond interactions with the target. This limited interaction profile is consistent with their lower docking scores and suggests reduced binding affinity toward EGFR.

Table 1: Molecular docking scores and key binding interactions of studied compounds with selected target proteins (PDB ID: 1M17)

Ligands	Docking score (Kcal/mol)	Active site residues (Distance Å)	Types of interaction
T1	-6.927	MET742 (3.39) ASP831 (3.48) LYS721 (4.18)	H-donor H-acceptor Pi-H
T2	-7.236	GLN767 (3.01), GLU738 (3.05) MET769 (3.31), MET769 (3.45) VAL702 (4.48)	H-donor H-acceptor Pi-H
T3	-5.911	GLN767 (2.96) THR830 (3.36), MET769 (3.40)	H-donor H-acceptor
T4	-6.175	VAL702 (4.24)	Pi-H
T5	-7.213	GLN767 (3.01) THR830 (3.53), MET769 (3.42) LYS721 (4.28)	H-donor H-acceptor Pi-cation
T6	-6.076	ASP831 (2.95), MET769 (3.05) LEU768 (3.60), MET769 (2.91)	H-donor H-acceptor
T7	-6.379	VAL702 (3.90)	Pi-H
T8	-6.539	ASP831 (2.81) LYS721 (3.37)	H-donor H-acceptor

Compound T8 had a moderate docking energy of -6.539 kcal/mol and engaged in hydrogen bonding with ASP831 and LYS721. The nature of these interactions reveals a good balance between the polar and electrostatic components. Although the binding affinity is weaker than T2 and T5, the engagement of catalytically active residues implies that T8 could have decent inhibitory activity.

The observed variation in docking scores among the studied compounds can be further rationalized based on their electronic properties obtained from DFT calculations. Compounds such as T2 and T5, which exhibited superior binding affinity, possess moderate HOMO-LUMO energy gaps and balanced hardness/softness values. These features suggest an optimal combination of electronic stability and reactivity, facilitating effective charge transfer and non-covalent interactions with key amino acid residues in the EGFR active site. In particular, relatively higher HOMO energies may enhance electron-donating ability toward electron-deficient residues, thereby strengthening hydrogen bonding and electrostatic interactions.

3.2 Docking validation analysis

The reliability of the docking protocol was assessed by re-docking the co-crystallized ligand into the EGFR active site. The predicted binding pose of the redocked ligand was then compared with its experimentally reported conformation. The superimposition of the native and re-docked ligands within the binding pocket of EGFR showed a high degree of overlap (Figure 3). The RMSD value between the native and re-docked poses was calculated to be 1.612 Å, which confirmed the consistency of the docking methodology [29,30]. The obtained value of RMSD is within the generally acceptable threshold (< 2.0 Å), indicating reasonable agreement between the predicted and experimental binding poses. However, slight deviations may still influence the precision of docking predictions and should be interpreted with caution.

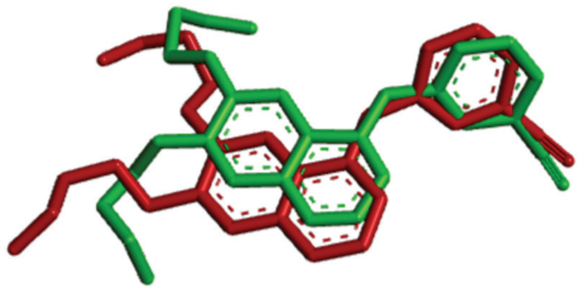

Figure 3: Superposition of native ligand (red) with docked ligand (green).

3.3 Density functional theory (DFT) calculation analysis

Density functional theory (DFT) calculations were carried out to examined the electronic characteristics and global reactivity parameters of the chosen 1,2,4-triazole-based Schiff base derivatives (T1-T8) (Figure 4). The orbital surfaces are represented using two colors (green and red), which indicate opposite phases of the molecular wavefunction, while the spatial distribution reflects the electron density regions involved in molecular interactions. The calculated HOMO energy levels were found in the range of -5.823 to -5.358 eV (Table 2). This suggests that the studied compounds have a reasonable tendency to donate electrons. Among them, compound T5 and T6 showed higher HOMO energies as compared to other tested compounds. This implies a stronger electron-donating nature of T5 and T6. This may facilitate their interaction with the deficient electrons present in the active site of EGFR. On the other hand, the comparatively low values of HOMO energy was observed for T1 and T7. These low values of HOMO often associated with their high electronic stability. The LUMO energy values range from -2.446 to -1.766 eV. It may provide information regarding the ability of these molecules to accept electrons. Low values of LUMO energy, as found for T1 and T7, may show that these molecules possess a high ability to accept electrons. It may facilitate the interaction of these molecules with amino acid residues present in the binding site. This type of donor-acceptor feature is considered beneficial for kinase inhibitors. This is because ligand-receptor binding is influenced by a combination of noncovalent forces. The energy difference between the HOMO and LUMO energy levels (ΔE), was calculated to range from 3.377 to 3.900 eV. Such energy gaps are often used to measure the chemical reactivity and kinetic stability of a compound. Compounds T1 and T7 showed a comparatively low ΔE. This indicated that they possess high reactivity and polarizability. Meanwhile, T4 demonstrated a high ΔE value, consistent with high electronic stability. In general, the moderate ΔE values calculated for the series represent a proper balance between molecular stability and reactivity, a factor that may be significant when considering drug-like compounds.

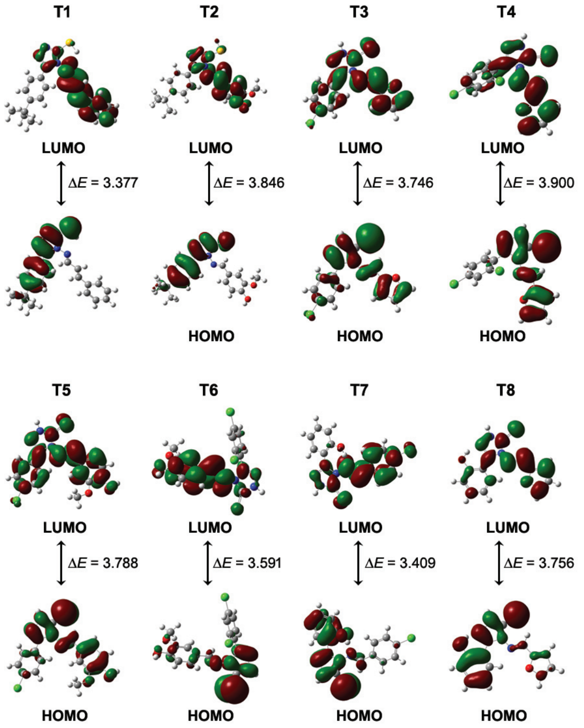

Figure 4: Comparison of band gap energy (eV) of the studied compounds (T1-T8)

The estimated chemical hardness (η) and softness (S) values (Table 2) of studied compounds provide further insights. Derivatives which have low hardness and high softness, especially T1, T6, and T7, could fit better with the electronic environment of the EGFR binding pocket. This characteristic could help facilitate favorable intermolecular interactions within the pocket. In addition, higher electrophilicity index (ω) values were observed for T1 and T7. This suggests a stronger electrophilic character, which could help facilitate better stabilization of charge-transfer interactions upon receptor binding.

The electronic descriptors obtained from DFT calculations show a meaningful correlation with the molecular docking results. Compounds with moderate HOMO–LUMO energy gaps (ΔE) tend to exhibit better binding affinity, as such values indicate a favorable balance between kinetic stability and chemical reactivity. Excessively high ΔE such as T4 corresponds to greater stability but reduced reactivity, which may limit effective interaction with the receptor. Conversely, compounds with relatively lower ΔE and higher softness (T1 and T7) are more polarizable but may lack optimal orientation or interaction strength within the binding pocket, resulting in moderate docking scores. Furthermore, electrophilicity index (ω) provides insight into the ability of ligands to accept electron density during binding. Compounds with moderate electrophilicity, such as T2 and T5, may achieve better stabilization through charge-transfer interactions with amino acid residues. These findings suggest that an optimal balance of electronic properties, rather than extreme values, is critical for effective ligand–receptor interaction.

Table 2: The variable quantum chemical parameters of the studied compounds

Compounds	E_{HOMO} (eV)	E_{LUMO} (eV)	ΔE (eV)	I (eV)	A (eV)	χ (eV)	μ (eV)	η (eV)	S (eV^{-1})	ω (eV)
T1	-5.823	-2.446	3.377	5.823	2.446	4.135	-4.135	1.689	0.296	5.062
T2	-5.699	-1.853	3.846	5.699	1.853	3.776	-3.776	1.923	0.260	3.707
T3	-5.715	-1.969	3.746	5.715	1.969	3.842	-3.842	1.873	0.267	3.940
T4	-5.742	-1.842	3.900	5.742	1.842	3.792	-3.792	1.950	0.256	3.687
T5	-5.554	-1.766	3.788	5.554	1.766	3.660	-3.660	1.894	0.264	3.536
T6	-5.358	-1.767	3.591	5.358	1.767	3.563	-3.563	1.796	0.278	3.534
T7	-5.823	-2.414	3.409	5.823	2.414	4.119	-4.119	1.705	0.293	4.975
T8	-5.763	-2.007	3.756	5.763	2.007	3.885	-3.885	1.878	0.266	4.018

3.4 Molecular electrostatic potential (MEP) map analysis

Molecular electrostatic potential (MEP) map is now become a highly applicable tool in modern drug design field [41]. Thus, the MEP maps of selected compounds (T1–T8) were analyzed to examine the charge distribution on the molecular surface (Figure 5) and to identify possible interaction regions with EGFR. In the MEP maps, red regions indicate areas of high electron density (negative potential), which are favorable for electrophilic attack, while the blue regions correspond to electron-deficient areas (positive potential), suitable for nucleophilic interactions. The green regions represent areas of near-neutral electrostatic potential. This color distribution helps in identifying the reactive sites of the molecules and understanding their interaction behavior with the target protein [42]. For all compounds, negative electrostatic potential was mainly found around the azomethine (–C=N–) nitrogen atoms, triazole ring nitrogens, and other heteroatoms such as sulfur and oxygen. These regions have the ability to act as hydrogen bond acceptors. Thus, it may be involved in the polar interaction with amino acid residues in the active site of EGFR. Molecules that have –OH or –OCH$_3$ functional groups (T2, T5, T6, and T8) have relatively higher electron density around these groups. This suggests their possible involvement in hydrogen bonding during binding. The positive electrostatic potential areas were primarily found on the -NH groups of the triazole ring and some aromatic hydrogen atoms. These regions can potentially act as hydrogen bond donor sites. Therefore, these area may participate in favorable interactions with the receptor. The availability of donor as well as acceptor sites implies that these compounds have the potential for forming stable non-covalent interactions with EGFR. Some variations were noted in the electrostatic distribution due to differences in substituents. Compounds which contain halogen substituent (T3, T4, T6, T7) had slightly polarized surfaces, especially near the phenyl rings. This may influence their binding orientation. Compounds with less bulky substituents exhibited a more uniform charge distribution, which may allow better flexibility during docking .

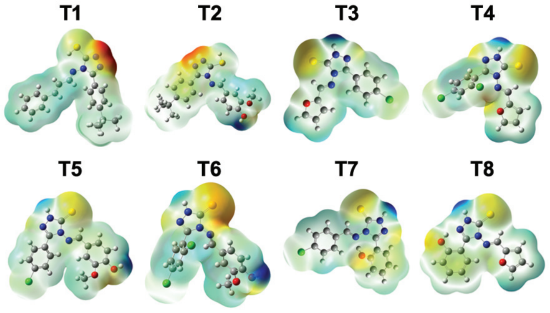

Figure 5: MEP maps of studied compounds.

3.5 *In silico* pharmacokinetics and toxicity analysis

3.5.1 Drug-likeness properties

Pharmacokinetic behavior evaluation is a critical step in identifying the potential of a compound as a candidate drug. In this research, the oral bioavailability of the proposed inhibitors was predicted by analyzing their drug-likeness properties based on Lipinski's Rule of Five. A compound is regarded as having acceptable oral absorption properties if it has a molecular weight of less than 500 Da, a logP value of no more than 5, fewer than five hydrogen-bond donors, fewer than ten hydrogen-bond acceptors, no more than ten rotatable bonds, and a topological polar surface area of less than 140 Å^2 [43, 44]. As shown in Table 3, the studied 1,2,4-triazole Schiff bases did not violate Lipinski's rule of five, which means that they have desirable drug-likeness properties. This result indicates that the chosen compounds have physicochemical properties suitable for orally available drug candidates, thus warranting further *in silico* screening for the EGFR target.

Table 3: Physicochemical properties of the selected compounds

Compounds	**LogP**	**HBD**	**HBA**	**TPSA (Å^2)**	**nrotb**	**MW**
T1	4.78	0	3	81.87	5	362.49
T2	3.95	1	5	111.33	5	382.48
T3	3.24	1	3	91.20	3	304.75
T4	3.75	1	3	91.20	3	339.20
T5	3.47	2	4	107.52	4	360.82
T6	3.98	2	4	107.52	4	395.26
T7	3.45	2	3	98.29	3	330.79
T8	2.28	2	4	111.43	3	286.31

LogP: logarithm of partition coefficient of compound between n-octanol and water, HBD: number of hydrogen bond donor, HBA: number of hydrogen bond acceptor, TPSA: Topological Polar Surface Area, nrotb: number of rotatable bonds, MW: Molecular Weight.

Table 4: Pharmacokinetic/ADME properties of selected compounds

Models	**T1**	**T2**	**T3**	**T4**	**T5**	**T6**	**T7**	**T8**
Water solubility (log mol/L)	-5.794	-4.766	-4.004	-4.202	-3.644	-3.736	-3.367	-3.888
Caco-2 permeability (log Papp in 10^{-6} cm/s)	1.567	1.29	1.29	1.321	0.993	1.141	0.815	0.879
Intestinal absorption (human) (% Absorbed)	91.225	89.641	91.25	90.104	89.086	87.933	92.229	90.038
Skin Permeability (log Kp)	-2.719	-2.75	-2.74	-2.74	-2.736	-2.737	-2.736	-2.764
P-glycoprotein substrate	Yes	Yes	Yes	Yes	Yes	Yes	Yes	Yes
P-glycoprotein I inhibitor	Yes	Yes	No	No	No	No	No	No
P-glycoprotein II inhibitor	Yes	Yes	No	No	Yes	Yes	No	No
VDss (human) (log L/kg)	0.165	-0.095	0.173	0.164	0.231	0.232	0.128	-0.064
BBB permeability (log BB)	0.482	-0.661	0.337	0.273	-1.448	-1.618	0.444	-1.163
CNS permeability (log PS)	-0.854	-2.046	-3.149	-3.157	-2.221	-2.1	-2.04	-3.257
CYP2D6 substrate	No	No	Yes	Yes	Yes	Yes	Yes	Yes
CYP3A4 substrate	Yes	Yes	Yes	Yes	Yes	Yes	No	Yes
CYP1A2 inhibitor	Yes	Yes	Yes	Yes	Yes	Yes	Yes	Yes
CYP2C19 inhibitor	Yes	Yes	Yes	Yes	Yes	Yes	Yes	Yes
CYP2C9 inhibitor	Yes	Yes	No	No	Yes	Yes	Yes	No
CYP2D6 inhibitor	No	No	No	No	No	No	No	No
CYP3A4 inhibitor	Yes	Yes	No	No	Yes	Yes	Yes	No
Total Clearance (log ml/min/kg)	0.127	0.19	0.057	0.173	-0.01	0.106	0.113	0.27

3.5.2 ADME analysis

The pharmacokinetic properties that are predicted for the eight 1,2,4-triazole Schiff base derivatives (T1-T8) indicate that these compounds have acceptable absorption characteristics (Table 4). It is noted that all these molecules have high intestinal absorption, which is above 87%. This property is a good measure of the potential oral bioavailability. It is consistent with their permeability across Caco-2 cells. The molecules possess moderate to high permeability, especially T1-T4. This suggests that these molecules are well-absorbed by the intestinal epithelial cells. Although these properties of absorption are desirable, the aqueous solubility of these molecules is low, as shown in Table 4, and varies from -3.367 to -5.794 log mol/L. Low aqueous solubility is normally observed in molecules that possess aromatic and heterocyclic rings. Aqueous solubility is a critical factor in determining oral bioavailability, as it directly influences drug dissolution in gastrointestinal fluids and subsequent absorption. Poor solubility can significantly limit the amount of drug available for absorption, even when membrane permeability is favorable. In the present study, the relatively low predicted solubility of the compounds may therefore represent a potential limitation, which could reduce their effective oral bioavailability and requires consideration in further optimization and formulation strategies.

All the tested molecules are predicted to be P-glycoprotein substrates. This indicates that P-glycoprotein is a significant property in the absorption of these molecules. P-glycoprotein is an efflux transporter that actively exports drugs from intestinal epithelial cells and other tissues, thereby reducing intracellular drug concentration. As a result, even compounds with good permeability may exhibit reduced oral bioavailability due to efflux back into the intestinal lumen. In addition, P-glycoprotein activity can limit tissue distribution and contribute to multidrug resistance, particularly in cancer therapy. However, only a few molecules, namely T1, T2, T5, and T6, are predicted to be P-glycoprotein inhibitors.

The calculated distribution parameters indicated that the VDss values were in the moderate range for most of the compounds. This reflects a balance between circulation in the plasma and distribution in tissues. The permeability of the BBB varied in the set of compounds. Compounds T1, T3, T4, and T7 were found to have relatively higher permeability. Compounds T5, T6, and T8 were found to have low permeability in the brain. For anticancer agents targeting peripheral proteins like EGFR, low permeability in the BBB is considered advantageous. This may minimize side effects in the CNS. The analysis of metabolism showed that most of these compounds are likely to be metabolized by CYP3A4. Inhibition of CYP1A2 and CYP2C19, which are members of the CYP family, was also noted in these compounds. This finding is pharmacologically significant, as these cytochrome P450 isoforms play an essential role in the metabolism of many clinically used drugs. Inhibition of these enzymes may lead to drug–drug interactions by reducing the metabolic clearance of co-administered drugs, potentially resulting in increased plasma concentrations and associated toxicity. Most importantly, none of these derivatives are likely to inhibit CYP2D6. This reduces the likelihood of serious drug–drug interactions. The calculated total clearance values were in the moderate range. This suggests that the derivatives may be metabolically stable and may not be rapidly cleared from the body.

The BOILED-Egg diagram (Figure 6) helps to visualize the gastrointestinal absorption and blood–brain barrier penetration of the compounds based on lipophilicity (WLOGP) and topological polar surface area (TPSA). In this model, the white region (egg white) represents compounds with a high probability of passive gastrointestinal absorption, whereas the yellow region (yolk) corresponds to compounds likely to penetrate the blood–brain barrier. All the investigated compounds were found to lie within the white area of the BOILED-Egg diagram. This indicates good gastrointestinal absorption probability. The results are also in accordance with the GI absorption values of the compounds. None of the compounds were found to lie completely within the yolk area of the diagram. This suggests poor penetration of the compounds across the blood–brain barrier. This observation are in agreement with the blood–brain barrier penetration values obtained from pkCSM, particularly for T5, T6, and T8, which fall outside the BBB favored zone. The BOILED-Egg analysis also supports the findings of the ADME studies by predicting good oral absorption and limited brain exposure of the compounds. This pharmacokinetic profile has important implications. Good GI absorption supports the potential for oral administration, which is a desirable property in drug development. On the other hand, limited BBB penetration may be advantageous for EGFR targeted anticancer agents, as it reduces the likelihood of central nervous system-related side effects. However, it may also restrict the effectiveness of these compounds in treating brain tumors or metastases. Therefore, the BOILED-Egg model highlights both the strengths (oral absorption) and limitations (restricted brain penetration) of the studied compounds.

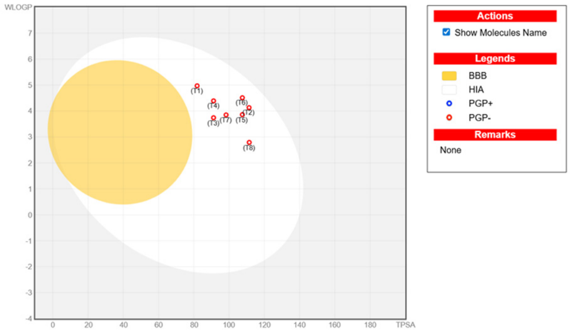

Figure 6: Boiled-egg diagram of studied compounds.

3.5.3 Toxicity prediction and safety profiling

The *in silico* toxicity evaluation of the selected 1,2,4-triazole Schiff base derivatives indicated that most of the compounds possess an acceptable safety profile, with some compound dependent variations (Table 5). In terms of mutagenicity, only compound T1 was predicted to be AMES-positive, while the remaining compounds (T2–T8) were predicted to be non-mutagenic. This suggests that the most of the derivatives may have a lower risk of genotoxic effects. The predicted maximum tolerated dose (MTD) values for humans were found to be within a moderate range for all compounds. Among them, compounds T5–T7 showed comparatively higher tolerated dose values. This may indicate a broader therapeutic margin. This trend was also supported by the acute oral toxicity predictions (LD_{50}), where all compounds fell within the low to moderate toxicity range. Similarly, the predicted chronic toxicity values (LOAEL) suggested that long-term exposure may be relatively better tolerated for compounds T5–T7 compared to the other derivatives.

Table 5: Toxicity profile of studied compounds

Parameters	**T1**	**T2**	**T3**	**T4**	**T5**	**T6**	**T7**	**T8**
AMES Toxicity	Yes	No	No	No	No	No	No	No
Max. tolerated dose (human) (log mg/kg/day)	0.209	0.222	0.207	0.332	0.613	0.662	0.697	-0.099
hERG I inhibitor	No	No	No	No	No	No	No	No
hERG II inhibitor	Yes	Yes	Yes	Yes	Yes	Yes	Yes	Yes
Oral Rat Acute Toxicity (LD_{50}) (mol/kg)	2.128	2.248	2.774	2.784	2.823	2.821	2.752	2.715
Oral Rat Chronic Toxicity (LOAEL) (log mg/kg_bw/day)	1.342	1.014	1.213	1.101	1.697	1.621	2.423	1.191
Hepatotoxicity	Yes	Yes	No	No	No	No	No	No
Skin Sensitisation	No	No	No	No	No	No	No	No

Cardiotoxicity analysis revealed that none of the compounds were predicted to inhibit hERG I. Although all compounds were predicted as hERG II inhibitors. Inhibition of hERG potassium channel is associated with delayed cardiac repolarization, which can potentially lead to QT interval prolongation and arrhythmias. Although hERG I inhibition is generally regarded as a stronger predictor of clinically significant cardiotoxicity, hERG II inhibition may still indicate a potential risk, particularly at higher concentrations or upon prolonged exposure. The uniform prediction of hERG II inhibition across all compounds suggests that this liability may be related to shared structural features, such as aromatic rings and heterocyclic moieties, which are commonly associated with interaction with the hERG channel. Therefore, this finding should not be overlooked, as it may impact the safety profile of these compounds during further development. However, it is important to note that *in silico* predictions of hERG inhibition are not definitive and may sometimes overestimate risk. Experimental validation using electrophysiological assays would be required to confirm the actual cardiotoxic potential. Additionally, structural optimization strategies such as reducing lipophilicity or modifying aromatic substituents may help mitigate this liability in future studies. while the predicted hERG II inhibition does not preclude further investigation of these compounds, it represents a significant safety concern that should be carefully addressed in subsequent experimental and optimization studies.

In terms of organ toxicity, it was found that the compounds T1 and T2 have the potential for hepatotoxicity. However, such risks were not observed for the other compounds. This finding indicates that some minor optimization of these compounds could lead to reduced toxicity related to liver. What is of significant interest is that none of the compounds tested were found to have the potential for skin sensitization. This indicates a favorable safety profile from a dermal toxicity perspective.

4 CONCLUSION

The current *in silico* study evaluated eight 1,2,4-triazole-derived Schiff bases for their ability to inhibit EGFR. Docking studies revealed that all eight compounds could bind to the EGFR active site, although with different binding affinities. T2 and T5 have shown better binding affinity compared to the other compounds. These compounds have shown good hydrogen bonding and electrostatic interactions with the active site residues namely MET769, GLN767, THR830, and LYS721. On the contrary, T3, T4, and T7 have shown low interactions with docking scores, indicating that their complexes with EGFR may be unstable. The docking studies were validated by density functional theory calculations.

The calculations revealed that the compounds have appropriate electronic properties including stability, reactivity, and charge distribution for biological interactions. Molecular electrostatic potential studies further validated the presence of distinct electrophilic and nucleophilic regions, as expected for their ability to interact with residues in the EGFR binding pocket. Pharmacokinetic and drug-likeness properties indicated that all compounds satisfy typical oral drug-likeness properties and have generally favorable absorption-related properties. Some variability was observed in predicted metabolism and toxicity among the derivatives.

Despite these promising findings, the study has certain limitations. The conclusions are entirely based on *in silico* approaches, and no *in vitro* or *in vivo* validation has been performed to confirm the biological activity and safety of the compounds. Moreover, molecular dynamics simulations, solvent-based DFT calculation, and more advanced free energy calculations were not included, which could provide deeper insights into the stability of ligand–protein complexes over time. The novelty of this work lies in the comprehensive computational investigation of previously synthesized 1,2,4-triazole-based Schiff bases against EGFR, combining molecular docking, DFT reactivity descriptors, and ADMET profiling in a unified approach. This integrated analysis provides valuable molecular-level insights into their potential as EGFR-targeted anticancer agents. Overall, while compounds T2 and T5 demonstrated relatively better computational performance, they should be considered as promising candidates for further experimental studies rather than definitive lead compounds. Future work should focus on experimental validation, structural optimization, and advanced simulation studies to confirm and extend the present findings.

Author Contributions

KB: Designed and executed all *in silico* investigations, formal analysis, data curation, visualization, and writing original draft of the manuscript;
BS: Conceptualization, supervision of the project, editing original draft, and project administration.

Conflicts of Interest

There are no conflicts to declare.

Data Availability Statement

The molecular docking, docking validation, and DFT calculation data generated in this study are available from the corresponding author upon reasonable request.

References

[1] Bhattarai N, et al. Anticancer Potential of Coumarin and Its Derivatives. Mini-Reviews in Medicinal Chemistry. 2021;21:2996-3029.

[2] Koya AI, Ibrahim SA. Carcinogenesis. In: StatPearls. Treasure Island (FL): StatPearls Publishing; 2025. .

[3] Tabti K, et al. Computational Assessment of the Reactivity and Pharmaceutical Potential of Novel Triazole Derivatives: An Approach Combining DFT Calculations, Molecular Dynamics Simulations, and Molecular Docking. Arabian Journal of Chemistry. 2014;17:105376.

[4] Zafar A, et al. Advancements and Limitations in Traditional Anti-Cancer Therapies: A Comprehensive Review of Surgery, Chemotherapy, Radiation Therapy, and Hormonal Therapy. Discovery Oncology. 2025;16:607.

[5] Garg P, et al. Emerging Therapeutic Strategies to Overcome Drug Resistance in Cancer Cells. Cancers. 2024;16:2478.

[6] Inamura K, et al. Is the Epidermal Growth Factor Receptor Status in Lung Cancers Reflected in Clinicopathologic Features? Archives of Pathology & Laboratory Medicine. 2010;134:66-72.

[7] Purba ER, et al. Activation of the EGF Receptor by Ligand Binding and Oncogenic Mutations: The “Rotation Model”. Cells. 2017;6:13.

[8] Herbst RS. Review of Epidermal Growth Factor Receptor Biology. International Journal of Radiation Oncology*Biology*Physics. 2004;59:S21-6.

[9] Bethune G, et al. Epidermal Growth Factor Receptor (EGFR) in Lung Cancer: An Overview and Update. Journal of Thoracic Disease. 2010;2:48-51.

[10] Li X, et al. Synthesis and Evaluation of Antitumor Activities of Novel Chiral 1,2,4-Triazole Schiff Bases Bearing γ-Butenolide Moiety. Organic and Medicinal Chemistry Letters. 2012;2:26.

[11] Ozcan I, et al. Novel 1,2,4-Triazole-Derived Schiff Base Derivatives: Design, Synthesis, and Multi-Enzyme Targeting Potential for Therapeutic Applications. Bioorganic Chemistry. 2025;157:108246.

[12] Aggarwal R, Sumran G. An Insight on Medicinal Attributes of 1,2,4-Triazoles.

European Journal of Medicinal Chemistry. 2020;205:112652.

[13] Almasmoum HA, et al. Synthesis and Multi-Target Antiproliferative Evaluation of Novel 1,2,4-Triazole-3-Thione Analogues against Breast Cancer: In Silico and in Vitro Mechanistic Insights. RSC Advances. 2025;15:24769-90.

[14] Ünver Y, et al. Synthesis of New 1,2,4-Triazole Compounds Containing Schiff and Mannich Bases (Morpholine) with Antioxidant and Antimicrobial Activities. Journal of Enzyme Inhibition and Medicinal Chemistry. 2016;31:89-95.

[15] Rao VS, Srinivas K. Modern Drug Discovery Process: An in Silico Approach. Journal of Bioinformatics and Sequence Analysis. 2011;2:89-94.

[16] Al-Mohaya M, et al. In Silico Approaches Which Are Used in Pharmacy. Journal of Applied Pharmaceutical Science. 2024.

[17] Khatiwada R, et al. In-Silico Analysis of Secondary Metabolites That Inhibit Aldose Reductase Targeting Diabetic Retinopathy. Journal of Institute of Science and Technology. 2025;30:197-209.

[18] Jakhar R, et al. Relevance of Molecular Docking Studies in Drug Designing. Current Bioinformatics. 2020;15:270-8.

[19] Mumit MA, et al. DFT Studies on Vibrational and Electronic Spectra, HOMO–LUMO, MEP, HOMA, NBO and Molecular Docking Analysis of Benzyl-3-N-(2,4,5-Trimethoxyphenylmethylene)Hydrazinecarbodithioate. Journal of Molecular Structure. 2020;1220:128715.

[20] Guan L, et al. ADMET-Score – a Comprehensive Scoring Function for Evaluation of Chemical Drug-Likeness. Medicinal Chemistry Communications. 2018;10:148-57.

[21] Aryal P, Shakya B. Synthesis, Cytotoxicity, Antibacterial and Antioxidant Activity of New 2-Substituted Benzimidazole Containing 1,2,4-Triazoles. Journal of Nepal Chemical Society. 2023;43:34-45.

[22] Devkota K, et al. Synthesis and Evaluation of Schiff Bases of 4-Amino-5-(Chlorine Substituted Phenyl)-4H-1,2,4-Triazole-3-Thione as Antimicrobial Agents. Journal of Nepal Chemical Society. 2020;41:26-35.

[23] Kapri KP, Shakya B. Synthesis, Characterization and Antimicrobial Evaluation of Schiff Bases of 4-Amino-5-(4-Tert-Butylphenyl)-4H-1, 2, 4-Triazole-3-Thiol. Journal of Nepal Chemical Society. 2018;39:1-9.

[24] RCSB Protein Data Bank. RCSB PDB: Homepage; 2026. Accessed: 2026-01-21. https://www.rcsb.org/.

[25] Khelfaoui H, et al. Molecular Docking, Molecular Dynamics Simulations and Reactivity, Studies on Approved Drugs Library Targeting ACE2 and SARS-CoV-2 Binding with ACE2. Journal of Biomolecular Structure and Dynamics. 2021;39:7246-62.

[26] Anighoro A, Bajorath J. Compound Ranking Based on Fuzzy Three-Dimensional Similarity Improves the Performance of Docking into Homology Models of G-Protein Coupled Receptors. ACS Omega. 2017;2:2583-92.

[27] Alomari FY, et al. QSAR Modeling, Molecular Docking and Cytotoxic Evaluation for Novel Oxidovanadium(IV) Complexes as Colon Anticancer Agents. Molecules. 2022;27:649.

[28] Shrestha A, et al. Molecular Docking and Dynamics Simulation of Several Flavonoids Predict Cyanidin as an Effective Drug Candidate against SARS-CoV-2 Spike Protein. Advances in Pharmacological and Pharmaceutical Sciences. 2022;2022:3742318.

[29] Hevener KE, et al. Validation of Molecular Docking Programs for Virtual Screening against Dihydropteroate Synthase. Journal of Chemical Information and Modeling. 2009;49:444-60.

[30] Shim H, et al. Pose Classification Using Three-Dimensional Atomic Structure-Based Neural Networks Applied to Ion Channel–Ligand Docking. Journal of Chemical Information and Modeling. 2022;62:2301-15.

[31] Systèmes D. Free Download: BIOVIA Discovery Studio Visualizer; 2026. Accessed: 2026-03-20. https://discover.3ds.com/discovery-studio-visualizer-download.

[32] Kanagathara N, Nanmaran R. Illustration of Potential Energy Surface from DFT Calculation along with Fuzzy Logic Modelling for Optimization of N-Acetylglycine. Computational and Theoretical Chemistry. 2021;1202:113301.

[33] Abu-Melha S. Design, Synthesis and DFT/DNP Modeling Study of New 2-Amino-5-Arylazothiazole Derivatives as Potential Antibacterial Agents. Molecules. 2018;23.

[34] Ali AAS, et al. Design, Synthesis, Molecular Modeling, Anticancer Studies, and Density Functional Theory Calculations of 4-(1,2,4-Triazol-3-Ylsulfanylmethyl)-1,2,3-Triazole Derivatives. ACS Omega. 2021;6:301-16.

[35] Hamadouche S, et al. Theoretical Design of New Grafted Molecules D-Glucosamine Oxyresveratrol-Essential Amino Acids: DFT Evaluation of the Structure–Antioxidant Activity. ACS Omega. 2024;9:37128-40.

[36] van de Waterbeemd H, Gifford E. ADMET in Silico Modelling: Towards Prediction Paradise? Nature Reviews Drug Discovery. 2003;2:192-204.

[37] Daina A, et al. SwissADME: A Free Web Tool to Evaluate Pharmacokinetics, Drug Likeness and Medicinal Chemistry Friendliness of Small Molecules. Scientific Reports. 2017;7:42717.

[38] Pires DEV, et al. pkCSM: Predicting Small-Molecule Pharmacokinetic and Toxicity Properties Using Graph-Based Signatures. Journal of Medicinal Chemistry. 2015;58:4066-72.

[39] Kamal MA, et al. Insights from the Molecular Docking Analysis of EGFR Antagonists. Bioinformation. 2023;19:260-5.

[40] Park JH, et al. Erlotinib Binds Both Inactive and Active Conformations of the EGFR Tyrosine Kinase Domain. Biochemical Journal. 2012;448:417-23.

[41] Wu S, et al. 1,2,4-Triazole-3-Thione Schiff Bases Compounds: Crystal Structure, Hirshfeld Surface Analysis, DFT Studies and Biological Evaluation. Journal of Molecular Structure. 2020;1219:128591.

[42] Kolodziejczyk W, et al. Conformational Analysis of Flephedrone Using Quantum Mechanical Models. Journal of Molecular Modeling. 2013;19:1451-8.

[43] Roskoski R. The ErbB/HER Family of Protein-Tyrosine Kinases and Cancer. Pharmacological Research. 2014;79:34-74.

[44] Varma MV, et al. Functional Role of P-Glycoprotein in Limiting Peroral Drug Absorption: Optimizing Drug Delivery. Current Opinion in Chemical Biology. 2006;10:367-73.